Two-Dimensional Optical Lattice Solitons

Nikolaos K. Efremidis,[1] Jared Hudock,[1] Demetrios N. Christodoulides,[1] Jason W. Fleischer,[1,2]
Oren Cohen,[2] and Mordechai Segev[2]
[1]*School of Optics/CREOL, University of Central Florida, Florida 32816-2700, USA*
[2]*Physics Department, Technion-Israel Institute of Technology, Haifa 32000, Israel*
(Received 16 April 2003; published 21 November 2003)

We study various families of two-dimensional discrete or lattice solitons, and show that they are possible only when their power level exceeds a critical threshold. In addition, we show that gap-lattice solitons exist only when the lattice possesses a complete 2D band gap. Our results suggest that these conditions are universally valid, irrespective of the nature of the nonlinearity or the specific structure of the index lattice. The analysis explains fundamental aspects of behavior of two-dimensional discrete solitons that have been very recently observed in photosensitive optical crystals.

DOI: 10.1103/PhysRevLett.91.213906 PACS numbers: 42.65.Tg

Wave propagation in periodic lattices is known to exhibit several fundamental features that arise from the presence of allowed bands and forbidden gaps. One of the most intriguing outcomes of nonlinearity in such periodic systems is the existence of self-localized entities better known as discrete or lattice solitons (LS). This family of self-localized modes has recently attracted considerable attention in diverse branches of science such as biological physics [1], nonlinear optics [2], solid state physics [3], and Bose-Einstein condensates [4]. Thus far, nonlinear waveguide lattices [2,5] have provided the only fertile environment for the direct experimental observation and study of one-dimensional LS [6–8]. Yet, in spite of the progress made in the past few years in 1D topologies [6,9], very little is known regarding lattice solitons in higher dimensions, where they are expected to exhibit a much richer behavior [10].

Earlier this year, two-dimensional LS were reported for the first time [11]. In this experiment, two basic families of discrete solitons were demonstrated: in-phase lattice solitons under self-focusing conditions and π out-of-phase gap soliton states in a defocusing environment [11]. Surprisingly, in this experiment it was found that 2D gap LS are possible even in ''backbone'' lattices [shown in Fig. 1(b)] that totally lack an absolute potential minimum on site. These observations indicate that the transition from solitons in 1D lattices to those in higher dimensions is far from being simple. In view of this, several fundamental issues must be addressed. For example, what are the basic features of 2D LS and how do they differ from their 1D counterparts? What are the required band gap properties (partial or complete) for LS to exist? What lattices possess the appropriate band structure to support 2D LS?

In this Letter, we study various families of solitons in 2D square lattices and show that they are possible only when their power level exceeds a *critical threshold*. This is in sharp contradistinction to 1D LS for which no such threshold exists [12,13] and is closely associated with the stability of solitons in 2D lattices. In addition, we find that a full two-dimensional photonic band gap is required for a gap LS soliton to exist. Thus, only potentials that are deep enough can support LS. The properties as well as the parameters of the index potential lattice necessary to establish a full band gap are presented. Our results are in good agreement with the experimental observations of Ref. [11]. Our analysis provides valuable information for the experimental realization of discrete and gap LS in other types of 2D photonic lattices (waveguide arrays and arrays embedded in photonic crystal fibers) and in other physical settings such as Bose-Einstein condensates [14]. The results presented here are applicable to other types of lattices, such as hexagonal, etc.

We analyze two generic, experimentally feasible, types of lattices: a sinusoidal lattice and a backbone lattice. We study the linear properties (band structure) of these lattices and consider the two most common types of optical nonlinearities; namely, the (i) Kerr and the (ii) saturable nonlinearity. In the Kerr case, the evolution of the slowly varying amplitude of the light in a periodic array is described by the nonlinear Schrödinger equation:

$$i\frac{\partial\psi}{\partial z} + \frac{1}{2}\nabla_\perp^2\psi + V(x,y)\psi + \sigma|\psi|^2\psi = 0, \qquad (1)$$

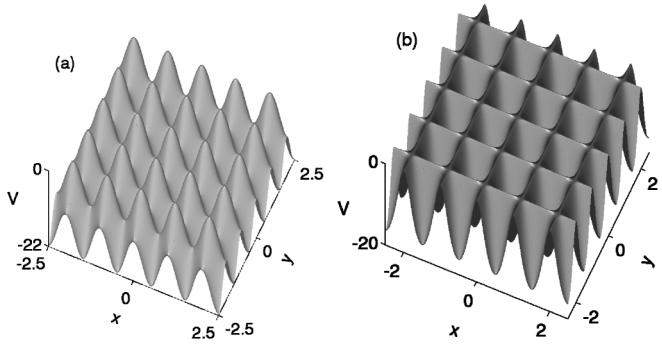

FIG. 1. Index potential of (a) a sinusoidal lattice and (b) of a defocusing backbone lattice when $A^2 = 1.21$.

where $\nabla_\perp^2 = \partial_x^2 + \partial_y^2$, $V(x, y)$ is a periodic index potential, $\sigma = \pm 1$ determines the nature of the medium nonlinearity (focusing/defocusing), and the field and coordinates in Eq. (1) have been normalized for convenience. For the purposes of this study, we assume that the 2D index potential is sinusoidal, e.g.,

$$V(x, y) = -(V_0/2)[\sin^2(\pi x) + \sin^2(\pi y)], \qquad (2)$$

where the period of the square lattice is 1 and V_0 is the index depression depth [see Fig. 1(a)]. Note that the linear eigenvalue problem associated with this potential is exactly solvable in terms of Mathieu functions [15].

For the saturable case, we assume a nonlinearity of the form $-1/(1 + |\psi|^2)$ that better suits the description of photorefractive crystals where 2D LS have been recently observed [11]. In this case, the waveguide lattice is optically induced and the nonlinear evolution equation for the optical soliton field ψ obeys a saturable nonlinear Schrödinger equation (see Ref. [16] for details):

$$i\psi_z + \frac{1}{2}\nabla_\perp^2\psi - \frac{V_0\psi}{1 + I(x, y) + |\psi|^2} = 0, \qquad (3)$$

where the normalized intensity pattern $I(x, y) = A^2\cos^2(\pi x)\cos^2(\pi y)$ is created through the interference of two pairs of laser beams that are coherently superimposed in order to establish an optical lattice. This intensity pattern is a 45° rotation of the expression $I(x, y) = (A^2/4)\{\cos[\pi(x + y)] + \cos[\pi(x - y)]\}^2$ of Ref. [11]. The potential depth as well as the sign and magnitude of the nonlinearity can be controlled by V_0, which is proportional to the voltage applied to the photorefractive crystal. In Eq. (3), under linear conditions, the index potential $V(x, y)$ is given by [17]

$$V(x, y) = -V_0/[1 + I(x, y)]. \qquad (4)$$

Figure 1 depicts the lattice potentials of interest. Figure 1(a) shows the potential of Eq. (2) and has the same structure for both the focusing and defocusing Kerr nonlinearity. The focusing case for the photorefractive nonlinearity has a similarly modulated potential and is not shown. The potential for the defocusing saturable nonlinearity of Eq. (4) is shown in Fig. 1(b). Note that, unlike the lattice of Fig. 1(a), which exhibits absolute index maxima on site, the profile of Fig. 1(b) is considerably different. In this latter case, the index maxima are not isolated but instead are located along crossed ridges, thus forming a backbone structure, as clearly shown in Fig. 1(b).

To find the associated band structure, we assume that the linear versions of Eqs. (1) and (3) admit solutions of the form $\psi = \exp(-iqz)u(x, y)$. In this case, the following eigenvalue problem results: $qu + (1/2)\nabla_\perp^2 u + V(x, y)u = 0$. Following Bloch's theorem, the eigenfunction, $u_{\mathbf{k}}(x, y)$ can be written as $u_{\mathbf{k}}(x, y) = U_{\mathbf{k}}(x, y) \times \exp(i\mathbf{k} \cdot \mathbf{r})$, where $U_{\mathbf{k}}(x, y)$ is periodic (in $\mathbf{r}$) having the period of the lattice, $\mathbf{k} = \hat{\mathbf{x}}k_x + \hat{\mathbf{y}}k_y$ is its Bloch momentum, and $\mathbf{r} = \hat{\mathbf{x}}x + \hat{\mathbf{y}}y$. This eigenvalue problem is then solved numerically.

Figure 2(a) [2(b)] corresponds to the band structure of the potential shown in Fig. 1(a) [1(b)]. As can be seen, different bands in these structures can overlap with each other, restricting (or even eliminating altogether) the number of complete band gaps. This is a general property of 2D lattices and is in direct contrast to 1D arrays, which are generically associated with an infinite number of complete Bragg resonance band gaps. In two dimensions, the number of full band gaps depends on the properties of the specific potential (depth, period, and form).

Figure 3(a) shows the eigenvalue (energy) bands (depicted in shaded regions) as a function of the potential depth V_0 of Eq. (2). In this case, when the potential V_0 is less than 13.8, we find that no complete band gap exists. For greater values of V_0, an indirect full band gap opens up between the (π, π) $\mathbf{k}$ vector of the first Brillouin zone and the $(\pm\pi, 0)$, $(0, \pm\pi)$ $\mathbf{k}$ vectors of the second Brillouin zone. By increasing the potential depth further, a second band gap opens between the third and the fourth band when $V_0 \approx 40.7$. For even greater values of V_0, more band gaps start to form. For the Kerr optical lattice of Eq. (1), the refractive index modulation, Δ, is related to the normalized potential depth via $V_0 = (2\pi n_0 a/\lambda_0)^2\Delta$. As an example, for wavelength $\lambda_0 = 0.5$ μm, lattice spacing $a = 11$ μm, and refractive index $n_0 = 2.3$, the minimum value of Δ required for a complete band gap is equal to 1.37×10^{-4}.

The backbone potential of Fig. 1(b) exhibits different behavior. As we can see in Fig. 3(b), when the potential depth is less than 28.4 (and $A^2 = 1.21$) all the bands overlap, i.e., no complete band gap exists. Using the same parameters as in the previous example, this potential depth corresponds to $\Delta = 1.05 \times 10^{-4}$. On the other hand, for bigger values of V_0, one gap opens up between the first and the second bands. Unlike the sinusoidal lattice case, we find that no other band gaps emerge for even greater values of V_0. This seems to be a general

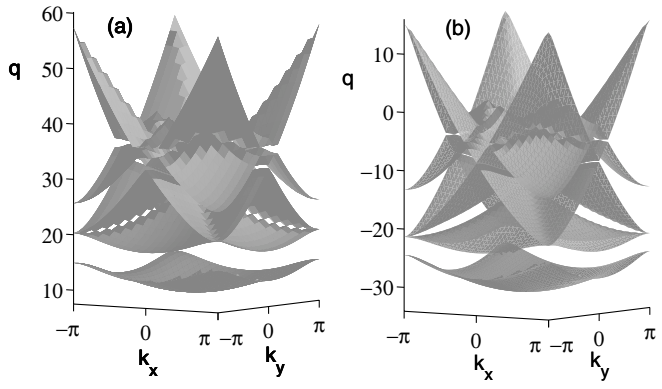

FIG. 2. Band structure corresponding to the lattice potential (a) of Fig. 1(a) when $V_0 = 21.6$ (b) of Fig. 1(b), for $A^2 = 1.21$, and $V_0 = -36.3$.

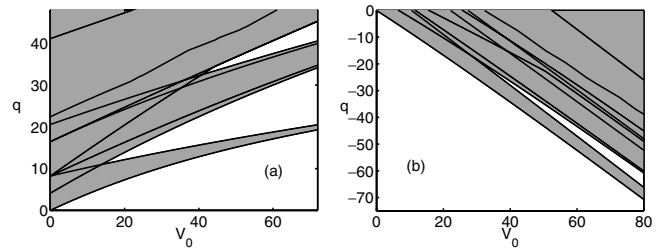

FIG. 3. Eigenvalue or "energy" bands as a function of the potential depth V_0 for (a) the sinusoidal lattice of Fig. 1(a) and (b) for the backbone lattice of Fig. 1(b).

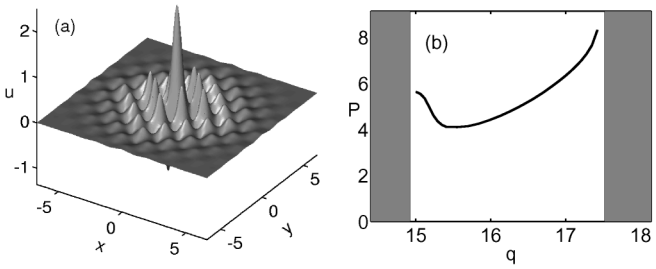

FIG. 5. (a) The field profile and (b) the associated $P - q$ curve for a Kerr self-defocusing gap LS with $V_0 = 21.6$.

feature of backbone lattices and results from the single-mode nature of this type of potential. The backbone structure resembles an array of ridge waveguides, where the effective refractive index at the center of every intersection is increased relative to other points on the grid. Waveguiding is weak at such a junction, and simulations of a single intersection (isolated "cross") show that the corresponding potential can support only a single bound mode and thus a single band gap. In principle, a gap can open up between two radiation bands, as it does in 1D structures [18], but we do not observe such a process in any 2D square lattice.

To find the lattice soliton solutions of Eq. (1) [and Eq. (3)], we first assume that $\psi(x, y) = u(x, y) \times \exp(-iqz)$. The resulting static or "time-independent" nonlinear Schrödinger equation is then solved numerically using relaxation methods. Two families of bright solitons were identified: self-focusing LS that exist in the semi-infinite band gap as well as self-defocusing LS that exist between the first and the second band.

Typical soliton structures for the Kerr nonlinearity and their corresponding existence curves are shown in Figs. 4 and 5 [19]. Theoretically, self-focusing 2D LS were first found in [16]. Subsequently, It was also shown that such structures can be induced by modulational instability [20]. The self-focusing (in-phase) soliton shown in Fig. 4(a) exists in the semi-infinite band gap below the first band. When its corresponding eigenvalue is close to the lowest energy band, the LS are broad, with the width of the soliton narrowing as the eigenvalue is lowered. In the self-defocusing case, represented by the π out-of-phase gap soliton [between bands 1 and 2 in Fig. 3(b)], this behavior is reversed. If its corresponding eigenvalue is close to its lower limit (the first band), the solutions are broad, whereas as the eigenvalue increases towards the second band, the LS get narrower. When the LS gets very close to the second band, its tails expand to occupy many lattice sites, and the LS itself exhibits a cusplike behavior. As in the focusing case, a complete band gap is always required; i.e., shallow potentials do not support LS. If the band gap is only partial (a situation not encountered in 1D or for focusing potentials), an input beam will radiate due to interaction with the linear spectrum in the transverse directions lacking a gap.

The power $P = \iint |u|^2 dx\, dy$ conveyed by the solitons versus the eigenvalue q is shown in Figs. 4(b) and 5(b). Note that there is a minimum power threshold required in order to observe a lattice soliton in two dimensions. In the 1D case, such a threshold does not exist [12,13]. We would like to mention that in the case of a semi-infinite band gap our results are in agreement with the discrete nonlinear Schrödinger case [21] as rigorously proven in [22].

The existence curves also give information on the stability of the solitons. For the focusing case, Fig. 4(b), the stability can be determined by a straightforward application of the Vakhitov-Kolokolov criterion [23]. More specifically, when $\partial P/\partial q < 0$, the solutions are stable, while close to the band $\partial P/\partial q > 0$ and the lattice solitons become unstable. This analysis cannot be applied directly to the defocusing case, Fig. 5(b), because gap LS represent higher order modes. For behavior close to the first band, the stability of these defocusing solutions can

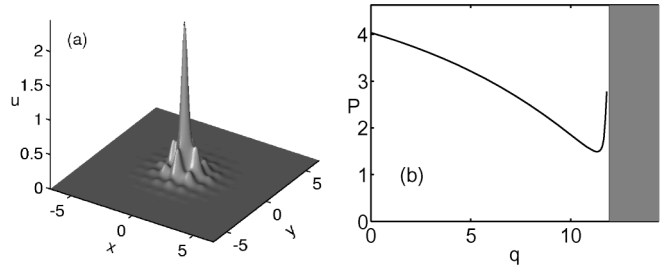

FIG. 4. (a) The field profile and (b) the associated $P - q$ curve for a Kerr self-focusing in-phase LS with $V_0 = 28.8$.

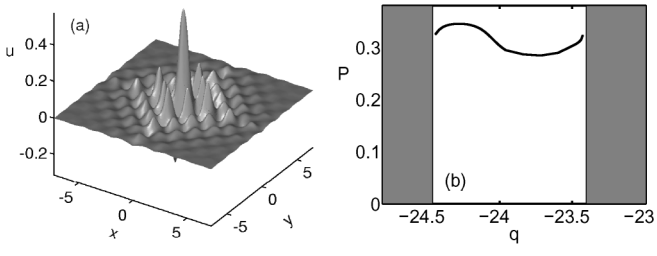

FIG. 6. (a) The field profile and (b) the associated $P - q$ existence curve for a photorefractive gap LS in a defocusing lattice for $V_0 = -36.3$.

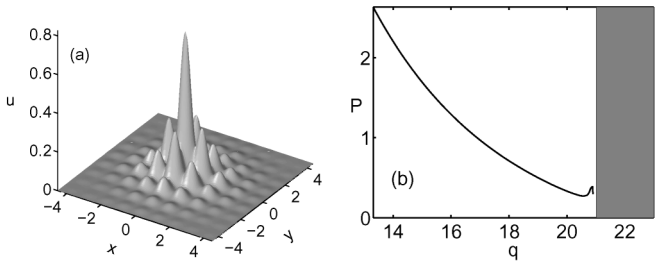

FIG. 7. (a) The field profile and (b) the associated $P - q$ existence curve for a photorefractive in-phase LS in a focusing lattice for $V_0 = 36.3$.

be studied using a Bloch envelope approximation (which cannot be applied close to the second band due to the mixed structure of the nonlinear mode). Close to the edge of the first band the LS are broad, so that they can be expressed as a periodic Bloch mode times a slowly varying envelope. This envelope obeys an effective nonlinear Schrödinger equation, to which the Vakhitov-Kolokolov criterion can be applied. As before, the defocusing nonlinearity gives us behavior that is opposite to the focusing case: Close to the first band (lower limit), $\partial P/\partial q < 0$ and the solution will be unstable, while increasing the eigenvalue to the regime where $\partial P/\partial q > 0$ will stabilize the solution. However, as the eigenvalue further increases, the soliton is affected by the second band and the solution ultimately becomes unstable again. We would like to mention that in a recent study gap LS in similar systems have been identified [24]. However, in contrast to these results [24], our analysis indicates that (i) a full 2D band gap is necessary for gap LS to exist and (ii) LS always exhibit power thresholds.

We find that the results obtained from the saturable model of Eq. (3) are in qualitative agreement with those obtained in the Kerr regime. In doing so, we have studied the backbone structure of Fig. 1(b). Figure 6(a) demonstrates a typical self-defocusing gap LS. In Fig. 6(b), the required power of such a soliton is depicted as a function of its eigenvalue. This curve has a minimum, although, due to the saturable nature of the nonlinearity, it is not as prominent as in the Kerr case. On the other hand, Fig. 7(a), shows a typical in-phase self-focusing LS (which occurs in a modulated lattice similar to the one in Fig. 1(a) [16]) and Fig. 7(b) depicts the total LS power as a function of q.

Finally, we would like to mention the connection between our results and Bose-Einstein condensates in an optical lattice [14]. In this case, Eq. (1) describes the evolution of the mean-field atomic condensate wave function ψ in a potential $V(x, y)$. The potential of Eq. (2) can then be created by the interference of two pairs of laser beams with orthogonal polarizations. A lattice similar to that of Fig. 1(b) can also be established when the two polarizations are parallel in a dark lattice. Using the normalizations of Ref. [13], one can show that for Rb^{87} atoms, and the lattice of Eq. (2) with 1.2 μm spacing, the potential depth required to create a band gap is approximately equal to 9.6 times the recoil energy. Also, in contract with the 1D case, a minimum number of atoms is always required to establish a LS.

This work is part of a MURI program on optical solitons and is also supported by the Israeli Science Foundation.

[1] A. S. Davydov and N. I. Kislukha, Phys. Status Solidi B **59**, 465 (1973).
[2] D. N. Christodoulides and R. I. Joseph, Opt. Lett. **13**, 794 (1988).
[3] W. P. Su *et al.*, Phys. Rev. Lett. **42**, 1698 (1979).
[4] A. Trombettoni and A. Smerzi, Phys. Rev. Lett. **86**, 2353 (2001); F. Kh. Abdullaev *et al.*, Phys. Rev. A **64**, 043606 (2001).
[5] D. N. Christodoulides, F. Lederer, and Y. Silberberg, Nature (London) **424**, 817 (2003).
[6] H. S. Eisenberg *et al.*, Phys. Rev. Lett. **81**, 3383 (1998).
[7] D. Mandelik *et al.*, Phys. Rev. Lett. **90**, 053902 (2003).
[8] J. W. Fleischer, T. Carmon, M. Segev, N. K. Efremidis, and D. N. Christodoulides, Phys. Rev. Lett. **90**, 023902 (2003); D. Neshev *et al.*, Opt. Lett. **28**, 710 (2003).
[9] F. Lederer *et al.*, in *Spatial Solitons*, edited by S. Trillo and W. Torruellas (Springer, New York, 2001).
[10] D. N. Christodoulides and N. K. Efremidis, Opt. Lett. **27**, 568 (2002).
[11] J. W. Fleischer, M. Segev, N. K. Efremidis, and D. N. Christodoulides, Nature (London) **422**, 147 (2003).
[12] P. J. Y. Louis *et al.*, Phys. Rev. A **67**, 013602 (2003).
[13] N. K. Efremidis and D. N. Christodoulides, Phys. Rev. A **67**, 063608 (2003).
[14] M. BenDahan *et al.*, Phys. Rev. Lett. **76**, 4508 (1996); B. P. Anderson and M. A. Kasevich, Science **282**, 1686 (1998).
[15] J. C. Slater, Phys. Rev. **87**, 807 (1952).
[16] N. K. Efremidis, S. Sears, D. N. Christodoulides, J. W. Fleischer, and M. Segev, Phys. Rev. E **66**, 046602 (2002).
[17] We would like to mention that the photorefractive nonlinearity is in general asymmetric and results to slightly elliptic LS. However, this small asymmetry does not change the fundamental properties of the soliton solutions discussed here.
[18] O. Cohen, T. Schwartz, J. W. Fleischer, M. Segev, and D. N. Christodoulides, Phys. Rev. Lett. **91**, 113901 (2003).
[19] Our results have been tested by changing the grid resolution of the relaxation algorithm until consistency is observed as well as with direct simulations.
[20] B. B. Baizakov *et al.*, J. Phys. B **35**, 5105 (2002).
[21] V. K. Mezentsev *et al.*, Sov. Phys. JETP Lett. **60**, 829 (1994); S. Flach *et al.*, Phys. Rev. Lett. **78**, 1207 (1997).
[22] M. I. Weinstein, Nonlinearity **12**, 673 (1999).
[23] N. G. Vakhitov and A. A. Kolokolov, Izv. Vyssh. Uchebn. Zaved. Radiofiz. **16**, 1020 (1973) [Radiophys. Quantum Electron. **16**, 783 (1973)].
[24] E. A. Ostrovskaya and Y. S. Kivshar, Phys. Rev. Lett. **90**, 160407 (2003).